Interpretation of the CABRI LT4 Test with SAS4A-code Analysis

March, 2001

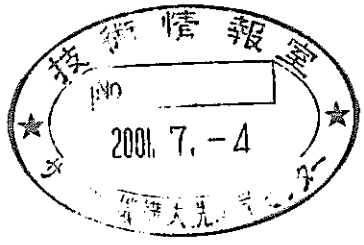

O-arai Engineering Center
Japan Nuclear Cycle Development Institute

〒319-1184　茨城県那珂郡東海村大字村松4-49
核燃料サイクル開発機構
技術展開部　技術協力課
Inquiries about copyright and reproduction should be addressed to :
Technical Cooperation Section,
Technology Management Division,
Japan Nuclear Cycle Development Institute
4-49 Muramatsu, Tokai-mura, Naka-gun, Ibaraki, 319-1184
Japan

JNC TN9400 2001-047
March, 2001

Interpretation of the CABRI LT4 test with SAS4A-code analysis

Y. Onoda[*1] and I. Sato[*1]

Abstract

The LT4 test was performed in the CABRI-FAST in-pile experiment program carried out in 1992~1995. The objectives of this test were to study the fuel pin failure mechanism and to observe the transient fuel motion within the pin and in the coolant channel.

The objectives of the present study are to clarify phenomena taking place in the experiment through data evaluation and SAS4A code analysis. Various experimental data have been analyzed with a help of SAS4A code calculation to interpret fuel pin failure mechanism and post-failure material relocation behavior.

Through this study, the rapid fissile elongation up to the fuel pin failure was recognized to have potential to delay the failure by about 50 ms, and probable effect of plenum gas to enhance dispersive fuel relocation has been recognized. And it was confirmed that SAS4A can reasonably simulate rapid molten-fuel ejection from failed fuel pin, rapid fuel relocation within the coolant channel assisted by the plenum-gas and the fuel freezing in the last part of transient.

---

*1 Advanced Technology Division, O-arai Engineering Center, JNC

JNC TN9400 2001-047
２００１年３月

SAS4A コード解析による CABRI LT4 試験評価

小野田雄一*　佐藤一憲*

要旨

CABRI LT4 試験は、中空燃料の ULOF (Unprotected Loss of Flow) 事故時の挙動研究を目的として 1997 年 3 月 11 日に実施された。本試験では、燃料ピンが過渡中に破損し、破損部からの溶融燃料の放出と、これに伴う冷却材流路のボイド化、及びボイド化流路中での燃料分散が観測された。本試験の破損後挙動評価に SAS4A コードを適用した。これにより、試験結果に対する現象論的理解が大きく深められた。また、中空燃料を用いた本試験での高いエネルギー破損条件における破損後挙動に対する SAS4A モデルの基本的適用性を確認した。さらに、本試験に用いた燃料ではガス・プレナムからの急速なガス放出が溶融燃料の放出挙動に影響を与えていることが認識された。この効果は燃料分散を加速する。従って、燃料設計に依存し、溶融燃料放出と分散の挙動をより正確に評価するためには、プレナム・ガス放出の影響を慎重に考慮する必要がある。

* 大洗工学センター、要素技術開発部、高速炉安全工学グループ

Contents

List of Figures

1. Introduction

The LT4 test is a TUCOP (Transient Under Cooling Over Power) test using the SCARABIX fuel in which the TOP was triggered during the LOF just before the coolant boiling. A structured TOP leading to an energy injection of 1.23kJ/g has been applied. There seems to have been significant pin bending during LOF as well as during TOP in this test. Coolant boiling took place about 400ms after the TOP triggering. A rapid fissile elongation was seen in a time range about 540 to 590 ms, which will have mitigated cavity pressurization and pin failure took place at 621 ms after TOP triggering when 80% of energy injection had been completed. Pin failure took place with significant fuel melting at a very high axial level of 630mmBFC (X/L=83%). After the pin failure, additional energy injection was quite limited.

The transient fuel behavior of this test has been studied in JNC using the PAPAS-2S code. Through this study, it was confirmed that the SCARABIX fuel had high PCMI(Pellet Cladding Mechanical Interaction) mitigation potential leading to the observed high failure-enthalpy level.

The post-failure behavior of this test has been studied using the SAS4A code focusing on fuel relocation and freezing within the coolant channel, which are important for reactivity consideration in the reactor evaluation. In this study, some part of the boundary condition for the post-failure calculation was adjusted based on the observed test result aiming at better investigation of the post-failure behavior on one hand, and effective verification of the SAS4A post-failure model on the other hand. Some important aspects of the LT4 test are presented in Chapter 2. Chapter 3 describes analytical condition and assumptions adopted in this study aiming at reflection of the information available from the experiment. Analytical results and discussion are given in Chapter 4.

The LT4 test was originary performed by IPSN out of the framework of the CABRI-FAST program. However, IPSN provided the test results for the CABRI partners and decided to include this test within the framework of the CABRI-FAST synthesis work which was a cooperative interpretation by the CABRI partners.

2. Some important aspects of the LT4 test

2.1 A rapid fissile elongation before the pin failure

In the LT4 test, a rapid and significant fissile elongation was seen before pin failure with the hodoscope, which caught upward fissile-fuel motion of about 47mm within about 50ms. The amount of fuel relocated beyond the original fissile region is estimated to have been around 20g(ref.1).

This rapid fissile elongation has two important aspects, which have potential to mitigate accident scenario. This rapid fissile elongation mitigates cavity pressurization, so that cavity pressurization-type pin failure can be significantly delayed or even prevented depending on the accident scenario. The delay of pin failure or prevention significantly reduces possibility of the LOF-driven-TOP, in which a coherent pin failure in the intermediate or outer-core region can lead to a high power burst. Another effect of this elongation is negative reactivity feedback, which has potential to affect the whole accident scenario.

Concerning the reactivity-feedback aspect, quantitative discussion based on the relative fuel worth, which is defined as described in Section 4.2, is effective. The relative-fuel-worth change due to the rapid fissile elongation cannot be calculated only from the mass increase above the fissile top but distribution of fuel-mass reduction within the original fissile region is necessary. However, hodoscope data, which is not sensitive to fuel mass reduction in the inner part, cannot provide reliable information on this point. An assumption that the relocated fuel corresponds to entire voiding of the PPN (Peak Power Node) region (see Fig.2-2) gives the highest relative worth reduction of 10%. On the other hand, an assumption that relocated fuel was supplied uniformly from the entire fuel cavity (cavity profile is taken from the SAS4A analysis), the relative worth reduction becomes 8.5%.

This rapid fissile elongation could be explained either by upward relocation of the uppermost solid fissile-fuel pellets or molten-fuel squirting into the above-fissile space through the central hole of the uppermost pellets. In any case, cavity pressure is the driving force and the rapid fissile elongation mitigates the cavity pressurization.

Although there is no direct evidence concerning the exact mechanism, information from the destructive examination suggests upward relocation of the uppermost fuel pellets. Such upward fuel relocation is likely to be followed by downward relocation after the pin failure due to in-pin gas flow from the upper plenum into the coolant channel through the failure rip. In accordance with this assumption, almost no fuel was found in the axial cut at the level just above the original fissile top. If molten fuel squirting was taking place, presence of some once molten fuel seems likely at this axial level.

2.2 Fuel pin bending effect

Based on the coolant-channel thermocouple data, fuel pin bending is recognized for the LT4 test during LOF and TOP. Although the hodoscope did not see any evidence of this bending, it is considered that the bending took place in the direction such that the hodoscope could not see it.

Under this bending, there was azimuthal temperature difference within the coolant channel and the first boiling seems to have taken place at one lateral part between 600mmBFC and TFC during TOP. Flow rate response shows that the coolant boiling initiation was rather mild, so that its exact initiation is not clear. However, meaningful sodium-void formation seems to have started at around 430ms and the global void volume increased monotonically in the later transient (Fig.2-2). At 430ms, the TC79 at TFC reached 950 ℃ while other TCs at the TFC level showed lower temperature, thereby indicating local boiling (see Fig.2-3). This local boiling region enlarged into the remaining azimuthal part up to 610ms (all TCs at TFC reaches 950 ℃) indicating initiation of bulk boiling at this axial level. However, enlargement of the boiling region from the initial part was much more enhanced in the axial direction rather than in the azimuthal direction. Local boiling region seems to have reached 600mmBFC at about 490ms already. Temperature of all three TCs at 600mmBFC reached 950 ℃ at about 570ms showing that occurrence of bulk boiling was earlier at this level than at TFC. This is because coolant-heating rate at 600 mmBFC is larger than that at TFC. At the time of observed pin failure, bulk boiling seems to have taken place between 600mmBFC and TFC at least.

Fig.2-4 illustrates the history of relative fuel worth during LOF and TOP evaluated from the hodoscope data. Fuel worth reduction is seen even before TOP

initiation, i.e., 0.95 during –4700 to 0 ms from the TOP triggering, and it becomes 0.90 during 0 to 539 ms after TOP onset. Fuel pin had been intact during these time intervals and no meaningful axial fuel-mass redistribution can be expected. Therefore, this worth reduction seems to have been caused by some unknown effect and the pin bending is regarded as a possible candidate for such effect.

2.3 Long-term fuel motion

In the LT4 test, the fuel-pin failure took place in a late part of TOP when 80% of energy injection had been completed, so that limited energy injection was performed after the pin failure. Because of the high failure enthalpy, rapid fuel ejection and relocation within the coolant channel took place. However, under the limited additional energy injection after failure, high fuel mobility could not be kept long due to heat transfer to the cold structure. Therefore, further fuel relocation at the last part of power transient was limited. It can be seen from the radiography and gamma-scanning data that dispersed fuel spreads between 100mmBFC and 900mmBFC within the coolant channel. Upward fuel-stub motion in the bottom of fissile column, which took place probably after the SCRAM, is also suggested by the radiography.

3. Special treatments for better simulation of the boundary condition

For better simulation of post-failure material-relocation behavior, realization of realistic boundary condition is indispensable. In this chapter, some special treatments and input-parameter selection used in this study to improve the boundary condition for simulation of the post-failure behavior are described.

Concerning the rapid fissile elongation, although the EJECT model had been under improvement, which could simulate the fuel-squirting event within its basic model framework with appropriate modifications, this study was performed in parallel to such activity. Therefore, the effect of rapid fissile elongation was included only with a simple specific treatment, in which cavity pressure at failure was corrected, without using the EJECT module.

3.1 Simulation of local boiling

A trial SAS4A analysis with the nominal coolant flow rate history resulted in good agreement of coolant-temperature history during LOF, but the coolant boiling during TOP was much later than the observation. As described in the previous chapter, the early coolant boiling in the experiment is considered to have been due to lateral variation of coolant temperature related to the pin bending. In order to compensate for this local effect, which is specific to the test condition, the coolant flow rate before the LOF was slightly reduced in the reference case. With this treatment, the boiling initiation and axial development of boiling region in the hottest lateral part can be better simulated. However, it should be kept in mind that this treatment leads to underestimation of liquid sodium remaining in the colder lateral part.

3.2 Simulation of mitigated cavity pressure due to the rapid fissile elongation

In the SAS4A model, definition of molten-fuel cavity region can be different between pre-failure phase and post-failure phase depending on objectives of each simulation phase. Because of this difference, gas distribution within the molten fuel cavity and the central holes above and below the melting region after the pin failure are not always equal to the pre-failure values. In the post-failure model, conserving the cavity pressure and the total gas amount for cavity and central holes, gas volume and gas mass in each axial segment are calculated.

Based on the interpretation of the LT4 experimental data given in Chapter 2, it is assumed that the cavity pressurization has been mitigated with an extra volume of 2.0 cc provided by the rapid fissile elongation. With this assumption, cavity pressure at pin failure will have been considerably reduced in reality. Therefore, the cavity pressure at failure lower than the nominal SAS4A result is specified in this study. With this option, gas mass for each axial segment in the molten-cavity region is unchanged but gas volume is adjusted within the code.

It should be noted that the total amount of gas within the cavity and that in the central holes above and below the melting region is conserved before and after the pin failure. This means that the difference of gas mass within the molten cavity is compensated for by the gas distribution within the central holes.

However, with the present post-failure model, gas within the central holes beyond the molten cavity region does not serve as a driving force for fuel ejection. In order to reflect the possible effect of gas distributed within the central holes as the driving force for fuel ejection, a special treatment is adopted in this study. In this special treatment, additional gas corresponding to the central hole one is released into all axial segments within the molten cavity region after the pin failure. The additional gas is supplied for each time step keeping the cavity pressure to the initial value as far as the gas is available.

3.3 Continued gas release from upper and lower gas plena

The CABRI-type Scarabix fuel used in the LT4 test had a 3 cm-long upper axial blanket above which 15 cc gas plenum was present. 0.869g of gas is assumed to have been within the upper plenum (pressure equilibrium at the end of LOF is assumed). During the cavity depressurization on fuel ejection, it is likely that the plenum gas flowed into the cavity. Furthermore, longer-time-scale gas flow into the cavity is also possible from the lower gas plenum.

In order to check the possible effect of such gas flow from the upper and lower gas plena, a special treatment is introduced in this study. In this special treatment, additional gas is supplied within the cavity nodes at the axial ends with different time scales. For the gas from the upper plenum to cavity, a very rapid gas flow to compensate for cavity-pressure decrease is given.

For the simulation of gas from the lower plenum of 9 cc, 0.957g of gas is released into the cavity with a time constant of 200ms simulating the probable delayed release.

3.4 Reduced initial heat transfer to steel on disruption

After the rapid molten-fuel ejection, cladding dry out region expands axially leading to fuel disruption. At this fuel disruption, the SAS4A model mixes the cold cladding as small particles with the hot molten fuel instantaneously. In reality, cladding surrounding the solid-fuel shell will be pushed outward on disruption, so that the complete mixing adopted in SAS4A will result in overestimation of initial heat

transfer to steel on disruption. Especially in case of the LT4 test, the limited energy injection after the molten-fuel ejection enhanced the effect of overestimated fuel heat loss on disruption.

In order to compensate for this overestimated heat loss, a large steel-droplet radius of 1 mm (usually 0.1mm) is adopted in this study, which leads to a delayed steel heat-up.

3.5 Correction for definition of moving fuel interface

In the LEVITATE module, velocities of upper and lower interfaces of the axially moving molten-fuel region are calculated with interpolation of molten fuel velocities at axial nodes just above and below the interface. However, for the axial node just above the upper interface of the moving molten fuel, velocity of molten fuel is not defined. With this definition, molten fuel velocity is zero at the node above the upper interface, so that the interpolation leads to zero velocity when the interface approaches the above axial node. In this study, velocity of the upper fuel front is assumed to be equal to that of the node just below the interface, in case of upward fuel movement.

The lower interface of the moving molten fuel is free from this type of trouble, because the velocity of the molten fuel at the node just below the lower interface is defined appropriately.

4. Analytical Results and Discussion

4.1 Before pin failure

Figs.4-1 and 4-2 show coolant-temperature increase during LOF and TOP respectively. It is intended in the analysis to simulate the local coolant boiling during TOP. The TC near the hottest azimuthal part increased faster than others indicating very local effect of pin bending during TOP. In order to simulate the coolant-boiling initiation in this hottest region, it was necessary in the analysis to have coolant temperature higher than the average TC data already during LOF. With this temperature bias in the analysis, initiation of the local boiling can be better simulated.

Figs.4-3 and 4-4 show coolant flow rate response and void volume respectively. The void volume is calculated from the flow meter signal before the pin failure. Although the coolant-boiling initiation seems slightly later in the analysis, void development after boiling initiation is faster in the analysis. Calculated upper and lower void interfaces are compared with experimental observation in Fig.4-5. Axial extent of coolant voiding at the pin failure is well simulated in the analysis. However, because of the one-dimensional model limitation, calculated void volume at pin failure is larger in the analysis than reality.

4.1.1 Calculated fuel pin condition at observed failure

Fig.4-6 shows calculated fuel-melting boundary, cladding temperature and cavity pressure distribution at the observed failure time. Significant fuel melting is seen at the observed failure location, although solidus fuel is remaining in the inner region with the CABRI-specific radial temperature inversion. Failure site is around the axial peak of cladding temperature.

In SAS4A, cavity pressure is not uniform along with the axial level. At the observed failure time, calculated cavity-pressure in the main cavity region is 215 bars and it decreases along with the central hole towards the axial ends. This calculated cavity pressure does not include the effect of the rapid fissile elongation, so that it is overestimated.

This axially non-uniform treatment for cavity pressure assumes non-equilibrium of pressure between the melting cavity and the central holes above and below it. If the pressure equilibrium is assumed, averaged cavity pressure decreases to 160bar. Such pressure equilibrium between the cavity and the central holes is very likely judging from the occurrence of the rapid fissile elongation. With the additional volume of 2.0cc corresponding to the rapid fissile elongation, averaged cavity pressure will further reduce to 70bar. Therefore, reflecting the effect of the rapid fissile elongation and probable pressure equilibrium, 70bar of cavity pressure is adopted as a reference condition for the post-failure evaluation.

In order to check appropriateness of this cavity pressure condition, the clad loading based on the thin-shell approximation is evaluated and compared with the mechanical testing data of irradiated 15-15Ti in Fig.4-7. The 15-15Ti data presented here corresponds to the strain rates of 0.1 and 1.0 (1/s), while the strain rate in a sample

SAS4A calculation for the cavity-pressurization phase of the LT4 test is 0.66 (1/s). In determination of the hoop stress, fractional melt radius is reflected. The hoop stress corresponding to 70 bar of cavity pressure seems to be considerably lower than the failure condition expected from the mechanical data. It seems likely that the SAS4A model is overestimating the gas volume within the cavity and/or underestimating the gas mass. Therefore, in order to check the possible effect of underestimated cavity pressure, a parametric case for post-failure calculation is performed. This parametric case is discussed later in this chapter.

Figure 4-7 can also be utilized for estimation of the effect of the rapid fissile elongation to delay the pin failure. With the present SAS4A model, gas-volume overestimation and/or gas-mass underestimation is expected, so that this aspect should be corrected. This means that the correction to the 70 bars of cavity pressure reflecting the effect of the rapid fissile elongation should shift this point into the mechanical-property band. On the other hand, if we apply a similar shift to the cavity-pressure loading without the effect of the rapid fissile elongation, failure condition is expected at around 570ms. This rough estimation suggests that the rapid fissile elongation has potential to delay the pin failure about 50ms. This delay results in 0.12 kJ/g of fuel enthalpy increase at PPN.

The conventional failure prediction in SAS4A based on cavity pressure and cladding temperature is given at 609ms and at the axial level of 580mmBFC. Although this prediction is not far from the real observation, it is only a combined result of absence of the rapid fissile elongation and underestimation of cavity pressure.

4.2 Post-failure material-relocation behavior

4.2.1 Effect of plenum gas transfer into the molten cavity after pin failure

Figures 4-5 and 4-8 present coolant-voiding behaviors with and without the possible effect of rapid plenum-gas transfer to the molten cavity after the pin failure respectively. Such gas transfer provides continued driving force for fuel ejection. Coolant flow rate response for these cases is compared in Fig.4-9. Without the plenum-gas transfer, the coolant flow rate observed in the experiment cannot be simulated at all. Void volume development evaluated from the flow rate measurement and the analytical result is presented in Fig.4-10. The good agreement between the

experimental observation and SAS4A result suggests that the assumption for plenum-gas transfer is reasonable.

On the other hand, it can be concluded from the experimental observation itself that the plenum gas transfer is the only possible explanation for the results. TCs in the coolant channel below 300mmBFC showed temperature below the sodium saturation during the void-development phase, so that the void consisted mainly of non-condensable gas. In the coolant channel above the failure site, ejected hot gas was not strongly cooled by sodium and structure, so that the TC showed temperature above saturation. Adopting a rough approximation for void-region pressure of 7bar and average temperature of 1000 degree C at 700ms, fission-gas mass within the void is estimated to have been about 1.2 g. This large amount of gas cannot be supplied only from the cavity, so that gas transfer from the plenum is indispensable. It should be noted that the upper gas plenum, which will have lower resistance for gas transfer to the cavity compared with that of the lower plenum, has about 0.9 g of fission gas.

In the following, plenum-gas transfer into the cavity is adopted in SAS4A analysis as the reference condition.

4.2.2 Development of coolant voiding, cladding dry out and fuel disruption regions

Development of coolant voiding, cladding dry out and fuel disruption regions are depicted in Fig.4-11. The void boundaries observed with the void detectors and flow meters are well simulated with the analysis. Initial cladding dry out is calculated in the analysis at around the observed failure time in accordance with the TC data suggestion. After the fuel ejection, although the dry out region expands rapidly in the analysis, direct comparison with the experiment is not easy. On the other hand, calculated fuel disruption well coincides with observed TC rupture especially in its propagation into the lower region.

4.2.3 Ejected molten-fuel relocation

Normalized fuel mass distributions for several time intervals are given in Fig.4-12. These fuel-mass distributions are corresponding to the average for each time window and they do not represent distributions at some instant.

Time interval of 575-654ms

In the time interval of 575-654ms, fuel-mass increase above TFC can be seen

in the experiment. This is considered to have been due mainly to the rapid fissile elongation and it is absent in the analysis. Although this rapid fissile elongation must accompany fuel mass reduction within the original fissile region, its localization is not easy from the data. The hodoscope data suggests a slight mass reduction in the middle and lower fissile part. However, because of the fact that fuel-mass reduction in the fuel inner part is often masked with the self-shielding effect, its relationship with the rapid fissile elongation is not clear. A slight cavity voiding due to fuel ejection is calculated with SAS4A providing a general agreement with the hodoscope data. Although fuel-mass increase is calculated in the upper half of fissile column, it cannot be clearly seen with the hodoscope. In the analysis, ejected fuel in the early ejection phase forms crusts on the structure and it can also be seen from the PTE around the failure location. It should be noted that the pin bending was taking place probably in the direction parallel to the hodoscope view. Possible initial fuel ejection into this direction may have resulted in less enhanced fuel-signal increase in spite of fuel accumulation there.

More precise hodoscope-data evaluation splitting the time interval into pre- and post-failure ones may help further discussion.

Time interval of 654-726ms

A significant amount of molten fuel was ejected from the pin within 100ms after the pin failure. Fuel voiding in the lower half of fissile column is slightly overestimated in the analysis. The adopted gas transfer may cause this from the lower plenum with the time constant of 200ms. As is shown in the later part of this section, the voiding of the lower fissile part is better simulated without this gas transfer in fact (see Fig.4-12 and 4-13, time interval of 654~726ms).

In the analysis, after fuel-crust formation, ejected fuel moves in both axial directions with an axial symmetry leading to a considerable fuel accumulation around the midplane. On the other hand, the experimental observation suggests mainly upward fuel relocation and evaluated fuel mass at the axial level of calculated fuel accumulation stays around the nominal value. This nominal-mass level seems to be a result of balance between fuel voiding within the cavity and additional fuel in the coolant channel. It is possible that a temporary fuel blockage was formed on the grid spacer just below the failure site with ejected molten and/or chunk fuel. Such fuel blockage may be formed at the very beginning of post-failure material relocation. This

hypothesis of temporary local blockage may be a possible explanation for the strange inlet flow rate response observed just after the pin failure, in which sudden interruption of downward slug ejection is included. Such temporary blockage may have lasted for a relatively long time.

In this time interval, fuel mass above TFC further increases with fuel penetration into the coolant channel above TFC. This fuel-penetration behavior above TFC is qualitatively well simulated in the analysis, although the quantity of penetrated fuel above TFC is slightly underestimated even with a correction for the effect of the rapid fissile elongation. The less pronounced upward fuel movement in the analysis may be cause by absence of the temporary blockage.

As described in Section 3.3, a parametric case without plenum gas effect on fuel ejection was performed. It can be seen from Fig.4-13 that without the help of gas flow from the gas plenum, fuel penetration into the upper part is much more underestimated. This result also supports the understanding that the rapid gas transfer from the plenum was taking place.

Time interval of 726-798ms

SCRAM was initiated at 720ms and 91% of energy injection was completed at 726ms. With this energy-injection history, further fuel relocation after SCRAM was small in the experiment. During this phase, SAS4A result shows enthalpy decrease of fuel within the coolant channel due to the heat loss to the structure without significant heat generation. With this enthalpy condition, material relocation becomes very slow in accordance with the hodoscope observation.

Time interval of 798-899ms

After SCRAM, as presented in the later part of this section, the relative fuel worth evaluated from the hodoscope data increases before 900ms. In this time period, fuel accumulation around the original TFC seems to have shifted downward on one hand, and fuel in the upper half of fissile column have relocated downward on the other hand. This downward relocation may be driven by gravity. Also in the analysis, fuel within the fissile region is slowly falling down with the gravity. However, the fuel accumulation in the upper part is sustained continuously in the analysis with remaining slight gas pressure. This gas pressure is highly dependent on the permeability of fuel accumulations against the gas flow. If depressurization of disrupted fuel region is responsible for the observed downward relocation of accumulated fuel around TFC, the

drag force presently used in the SAS4A model may be overestimated. Otherwise, thermal attack on the cladding structure in the gas-plenum region may have resulted in gas-discharge-pass formation in reality.

Time interval of 900-1700ms

After 900ms, upward relocation of the lower fuel stub was observed in the experiment, suggesting the gas within the lower plenum was not completely released up to this time. This information has provided the background for the assumption of 200ms time constant for gas transfer into the cavity from the lower plenum. The gas release from the lower plenum seems to have pushed the fuel accumulation around TFC again upward, so that the relative worth increase is cancelled.

4.2.4 Relative fuel worth

In the following, 'relative fuel worth', which is useful for reactor-case consideration is used. This parameter is defined with integration of local fuel mass multiplied by relative local power in CABRI along the fissile height. The initial relative worth is unity and fuel mass reduction from the fissile region leads to reduced relative worth proportionally. Fuel relocation within the fissile region from high power region to low power region also leads to relative worth reduction.

Relative fuel worth corresponding to the SAS4A analysis and hodoscope data is presented in Fig.4-14. Absence of fuel the rapid fissile elongation in the analysis makes direct comparison with the hodoscope difficult. In order to make the comparison effective, an additional line is introduced for the SAS4A result, in which a relative worth shift of –0.085 corresponding to the assumption of uniform cavity mass reduction is applied. Although -0.05 of relative worth reduction can be deduced for the time interval just before pin failure, this is not well representing the effect of the rapid fissile elongation.

The rapid fuel relocation within the cavity toward the failure site at the high axial level and dispersal within the coolant channel, as shown in Fig.4-15, results in -0.055 worth change during 620-650ms. The continued worth reduction after 650ms both in the analysis and experiment is caused mainly by channel fuel relocation into the above TFC region. It can be concluded that the short-term fuel worth change, which is important for the termination of the initiation-phase power transient in the reactor evaluation, can reasonably be simulated with the SAS4A model except for the effect of

the rapid fissile elongation.

After the SCRAM initiation, compressive fuel relocation under the reduced driving pressure for dispersive fuel relocation leading to a slight worth increase is observed both in the analysis and experiment. SAS4A can reasonably simulate the low mobility of the low enthalpy fuel in accordance with the reality. However, after 900ms, slight gradual fuel relocation leading to a small amount of worth reduction is taking place in the analysis. This shows that the frozen fuel in SAS4A still has minimum mobility, so that attention is necessary for reactor application especially for a long-term transient evaluation if a complete fuel blockage is concerned.

4.2.5 Effect of initial cavity pressure on post-failure fuel relocation

In order to check effects of assumed cavity pressure on post failure behavior, a parametric SAS4A case with a specified cavity pressure of 210bar is performed. With this different cavity pressure specification, gas mass is conserved and gas volume is reduced automatically. With the same gas-mass availability for fuel ejection, this case resulted in short-term fuel relocation quite similar to that of the case with 70 bars as shown in Fig.4-16. In these cases, the correction corresponding to the plenum-gas effect is not included, so that the driving force for fuel ejection commonly disappears at about 10-20ms after pin failure. However, comparison of these cases clearly shows that the effect of the initial cavity pressure on fuel relocation is not large. This result suggests that the uncertainty of the initial cavity pressure in the SAS4A model does not give large impact on post-failure fuel relocation.

5. Conclusion

1. Through the SAS4A analysis, the rapid fissile elongation up to the fuel pin failure in the LT4 test was recognized to have potential to delay the failure by about 50 ms, and lead to relative fuel-worth reduction of about 8.5%.
2. After the fuel pin failure, following aspects resulted in rapid initial fuel-worth reduction of about 14% within 100ms in addition to the above mentioned fuel elongation effect:
   - Cladding rupture at the high failure site (X/L=81%) leading to molten fuel relocation within the cavity from the middle part toward the high failure site, and
   - Mainly upward relocation of the ejected fuel within the coolant channel.
3. Through the present SAS4A analysis, probable effect of plenum gas to enhance dispersive fuel relocation has been recognized.
4. The better simulation of post-failure material relocation with the special treatment for the plenum-gas effect indicated the potential of SAS4A to simulate the plenum-gas-assisted fuel dispersal, although such behavior seems quite dependent on the pin design and accident scenario.
5. Because of the limited energy injection after the rapid post-failure material-relocation phase, material relocation settled down with fuel freezing and final fuel distribution was limited in 100 mmBFC ~ 900 mmBFC.
6. Present SAS4A can reasonably simulate the post-failure material-relocation behavior in the LT4 test consisting of rapid molten-fuel ejection from failed fuel pin, rapid fuel relocation within the coolant channel and the fuel freezing in the last part of transient.

Acknowledgement

The IPSN offer to have allowed the LT4 test results available for other CABRI partners within the CABRI-FAST synthesis work is greatly appreciated.
The authors also express their appreciation for Mr. Yoshiki SATO of Nuclear Engineering System Inc. and Mr. Takuhiro CHUBACHI of CSK Inc., who helped the analytical works and preparation of the figures.

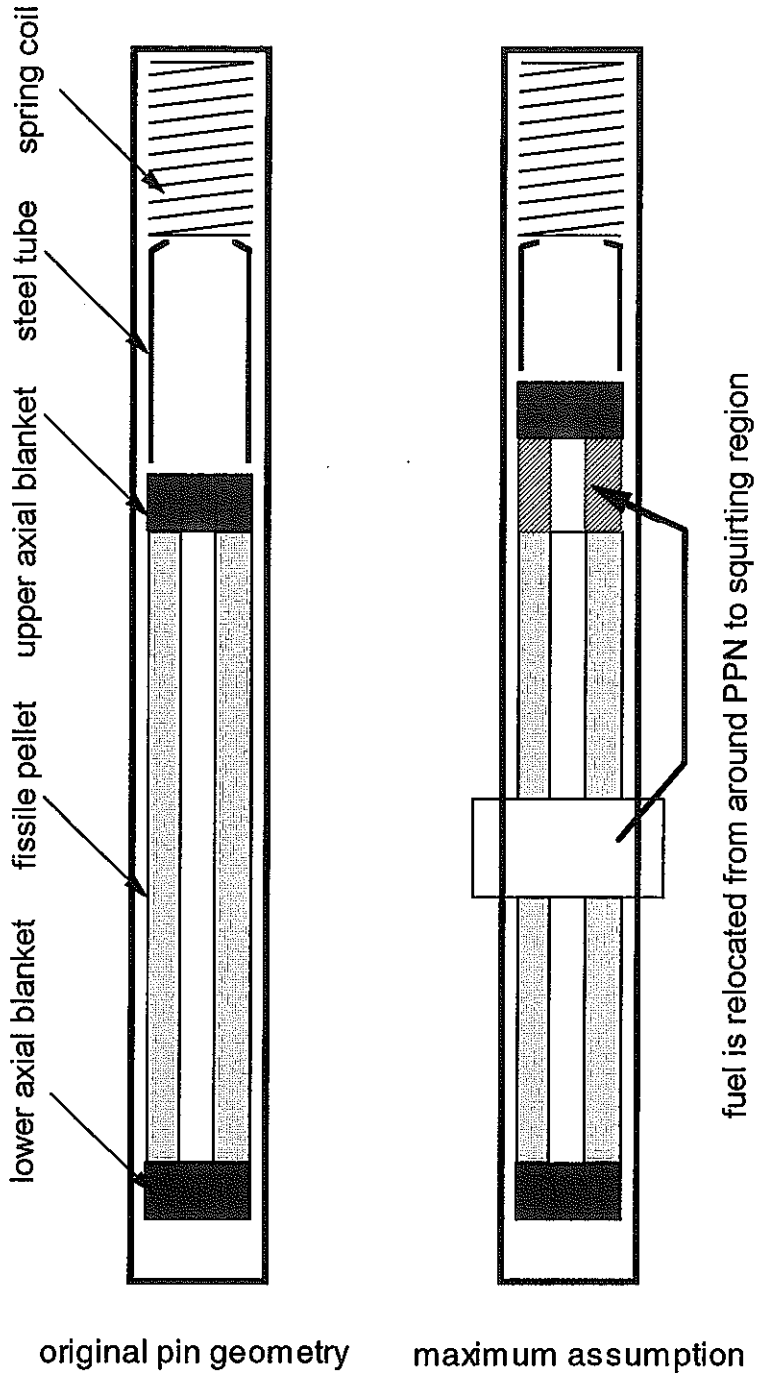

Fig.2-1 Assumption of fuel mass distribution within the original fissile region after fuel squirting

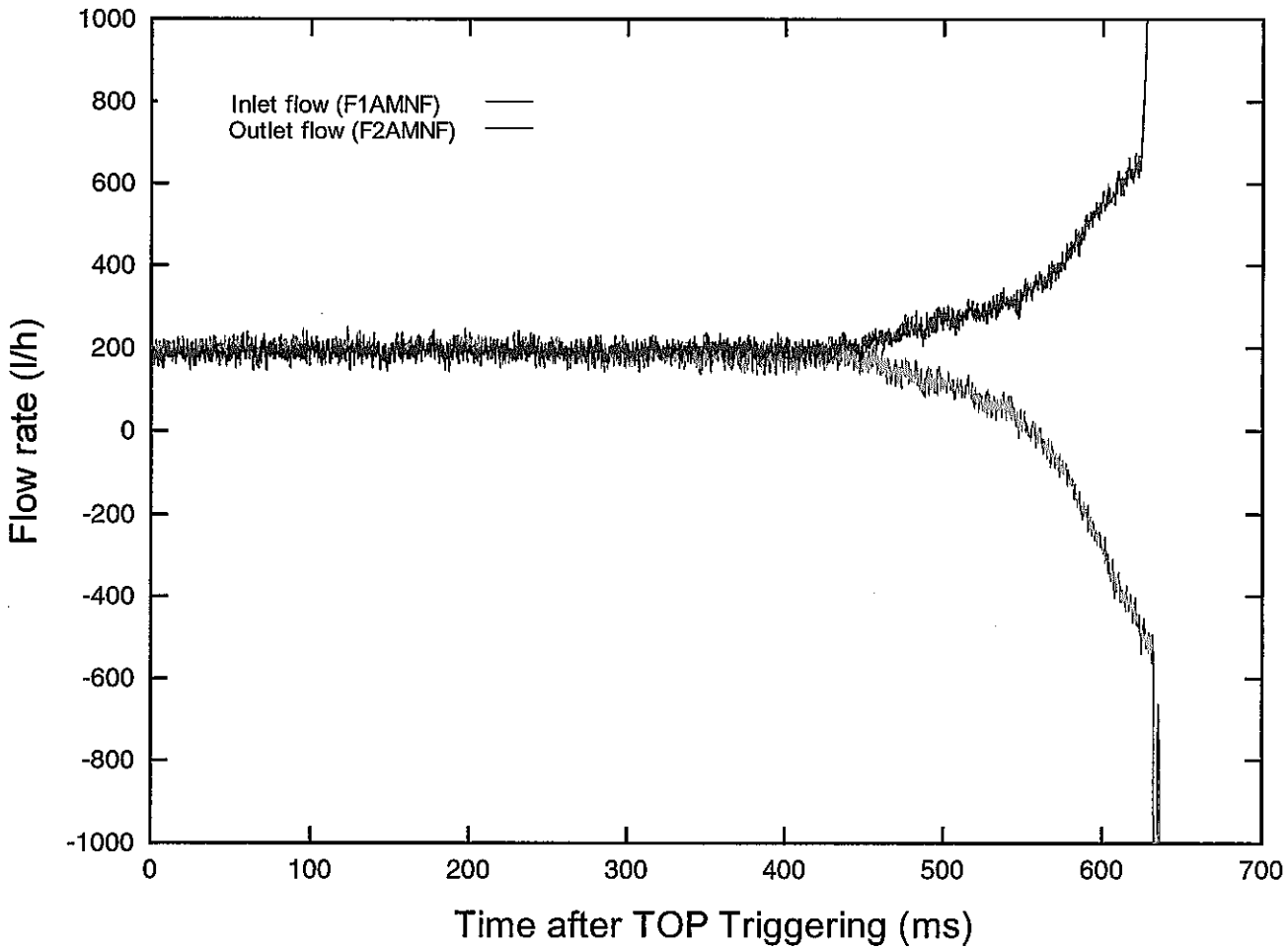

Fig.2-2 Coolant flow rate response during the TOP

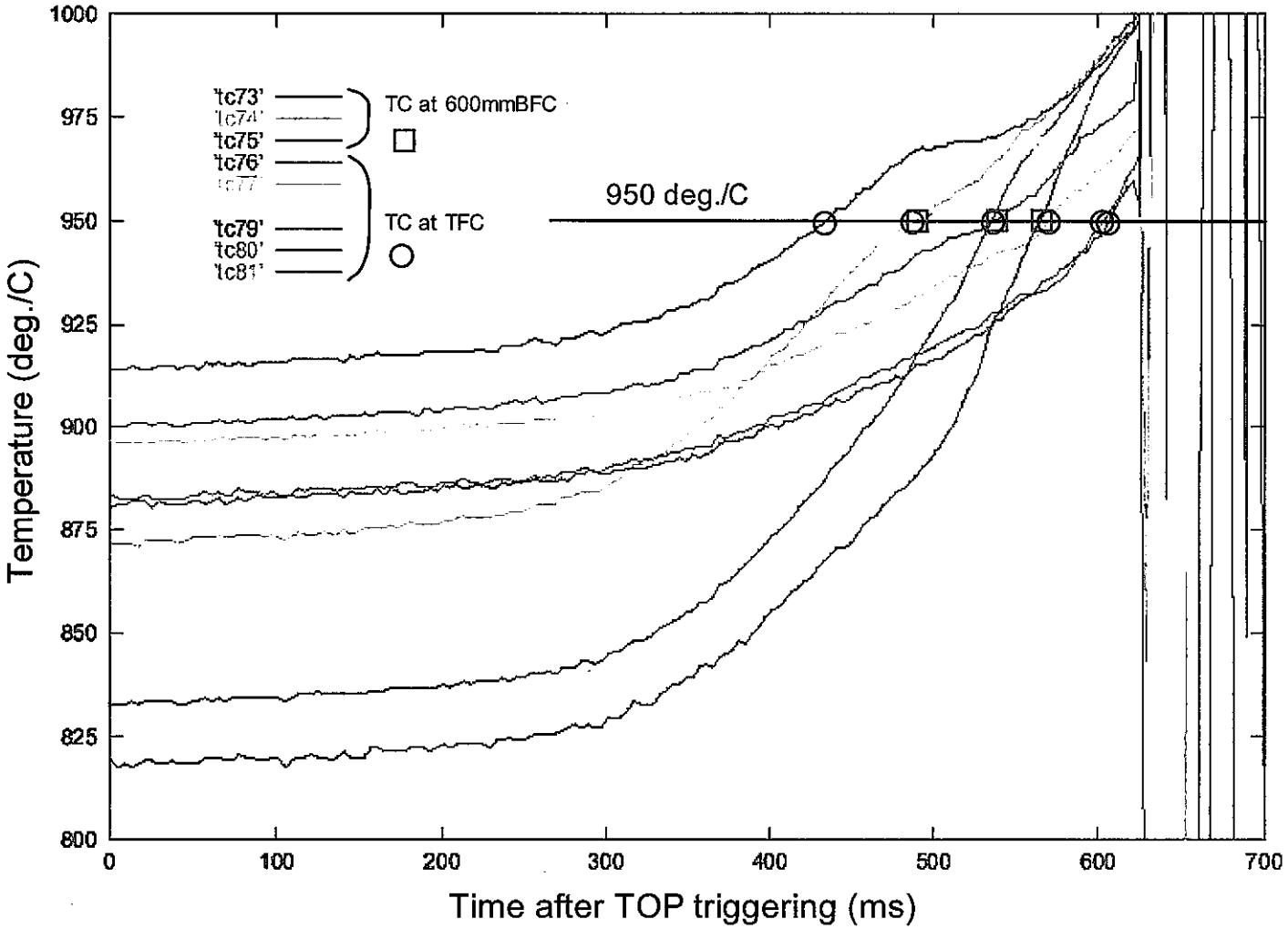

Fig.2-3 TC responses around boilling onset

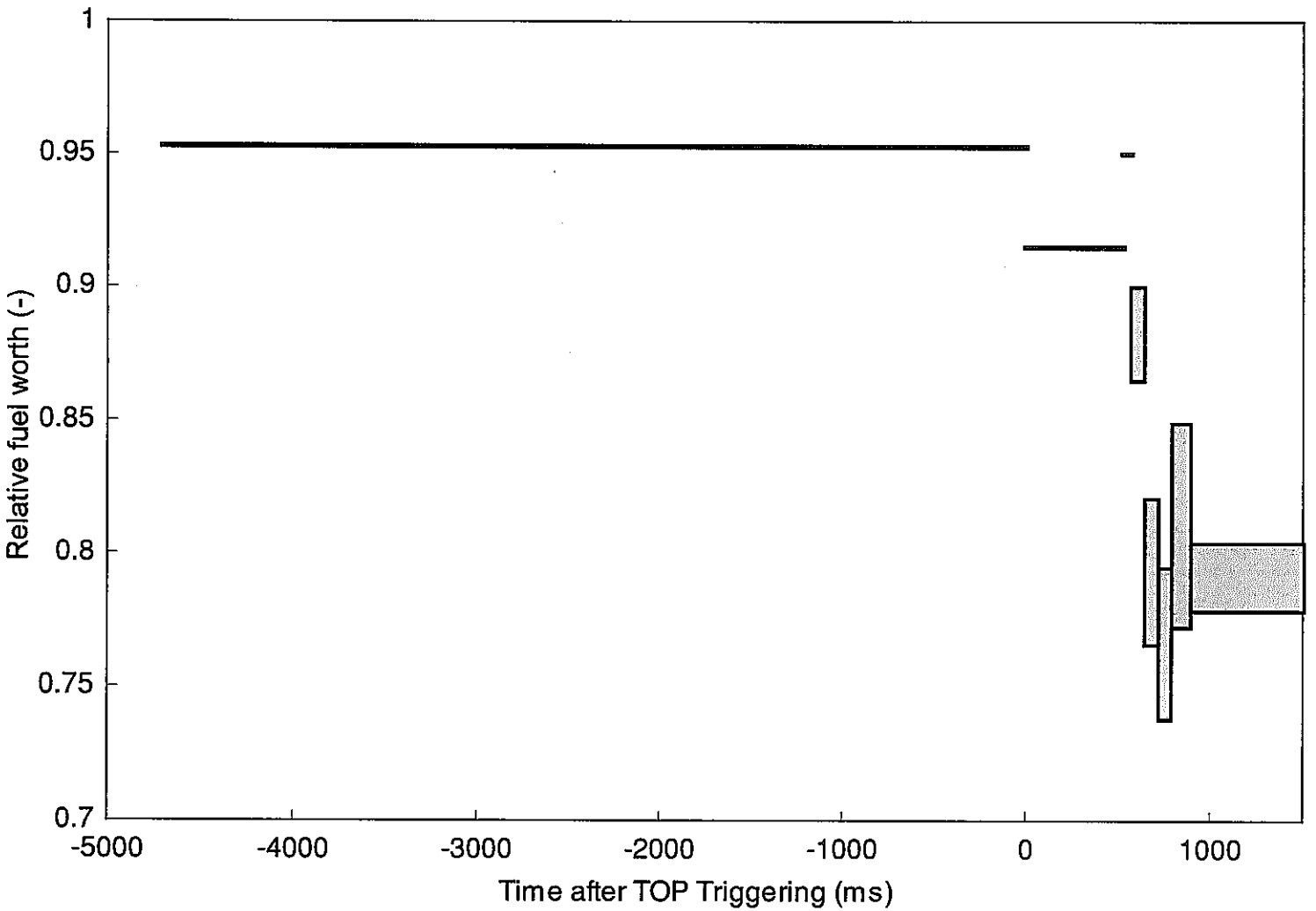

Fig.2-4 Histories of the relative fuel worth deduced from the hodoscope data

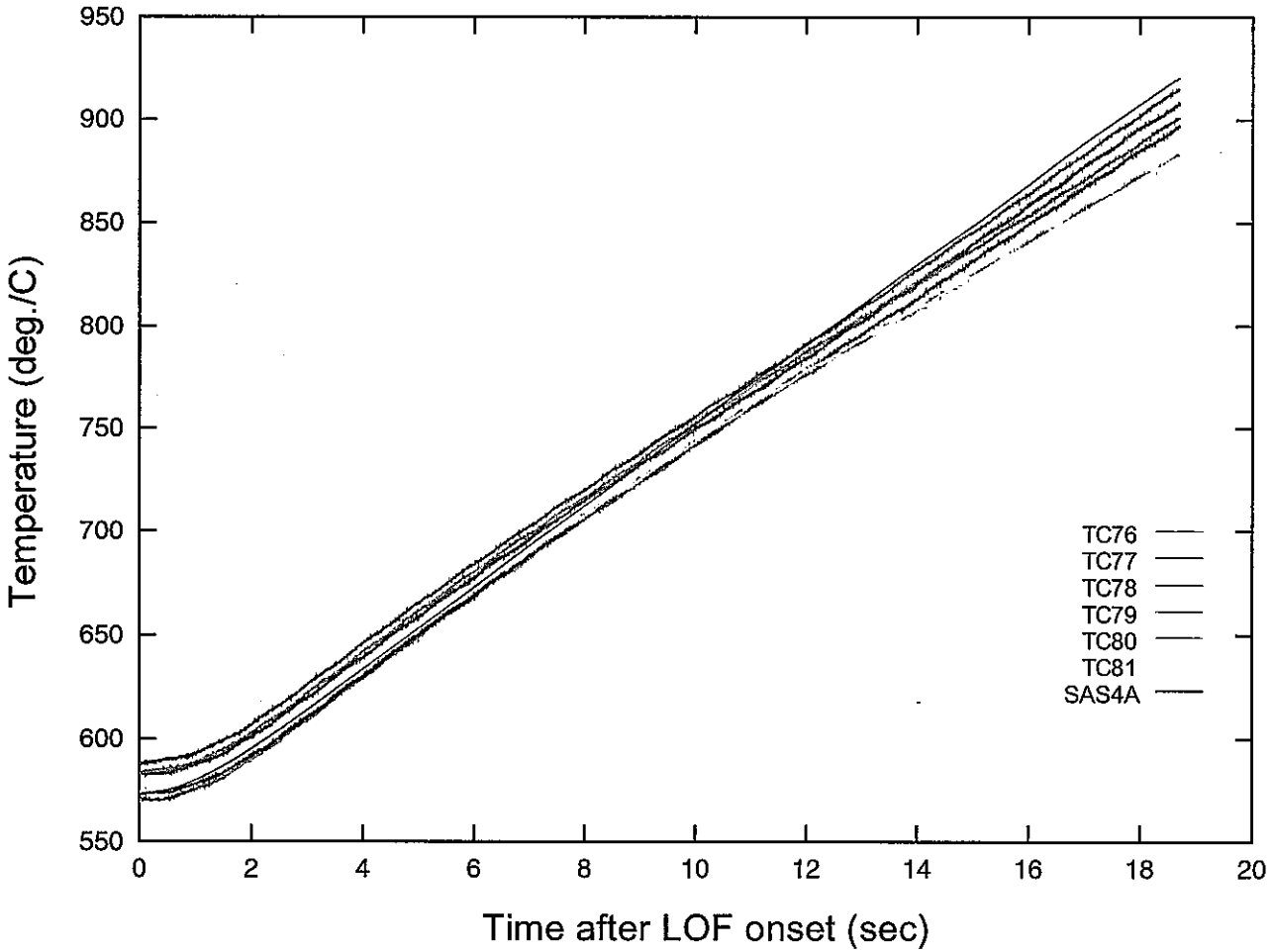

Fig.4-1 Coolant channel TC responses during the LOF

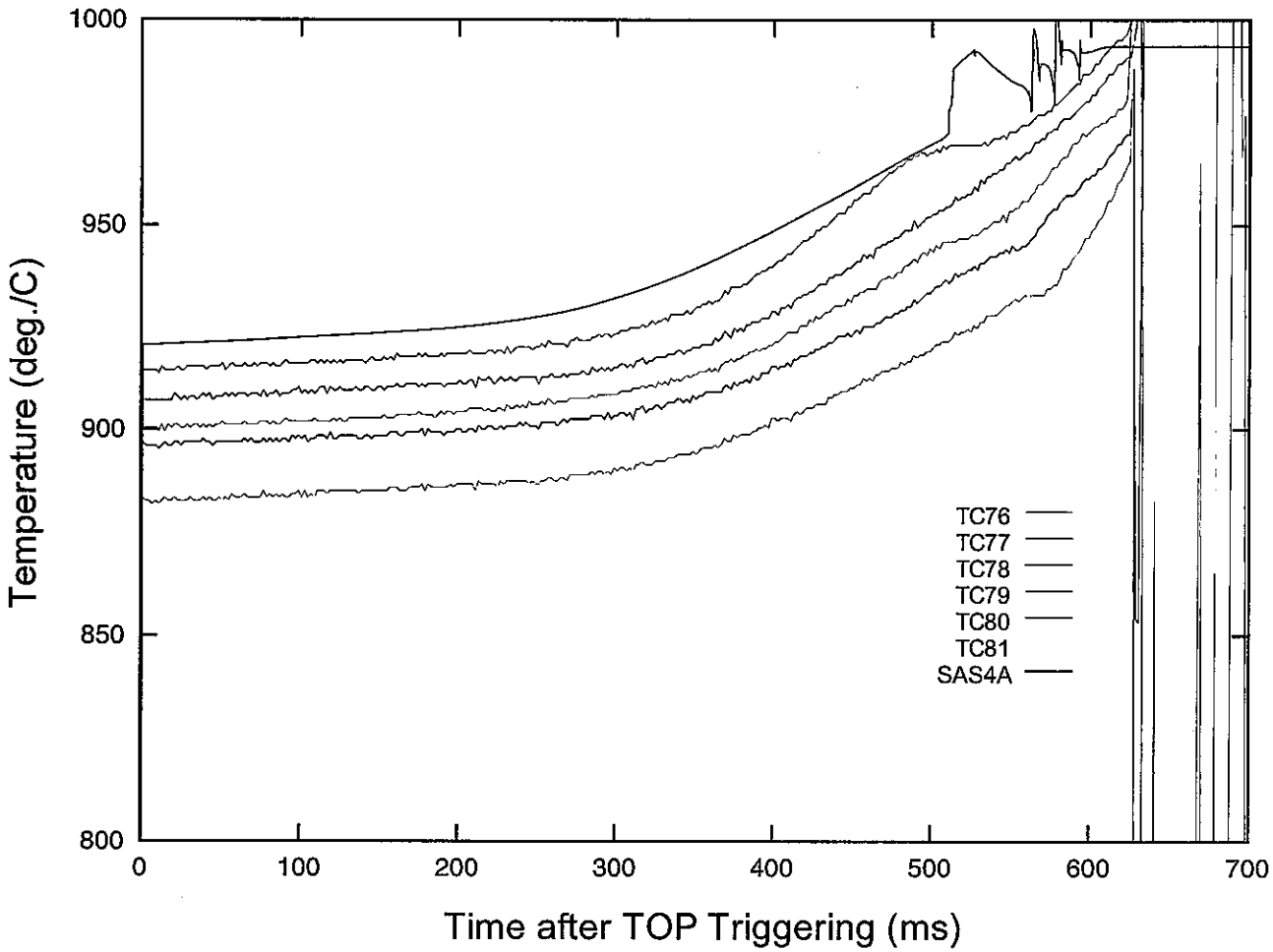

Fig.4-2 Coolant channel TC responses during the TOP

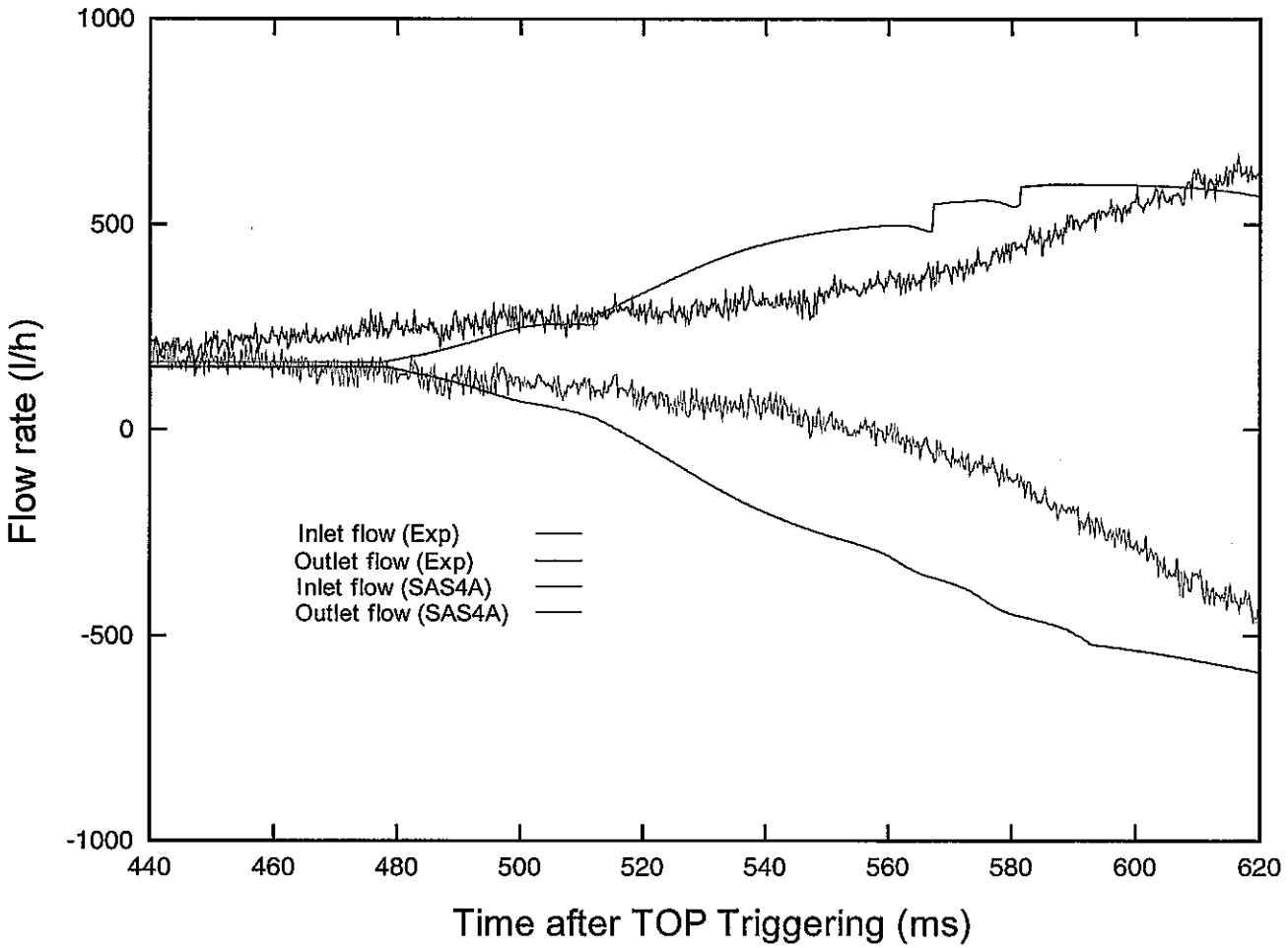

Fig.4-3 Comparison of coolant flow rate response during the TOP

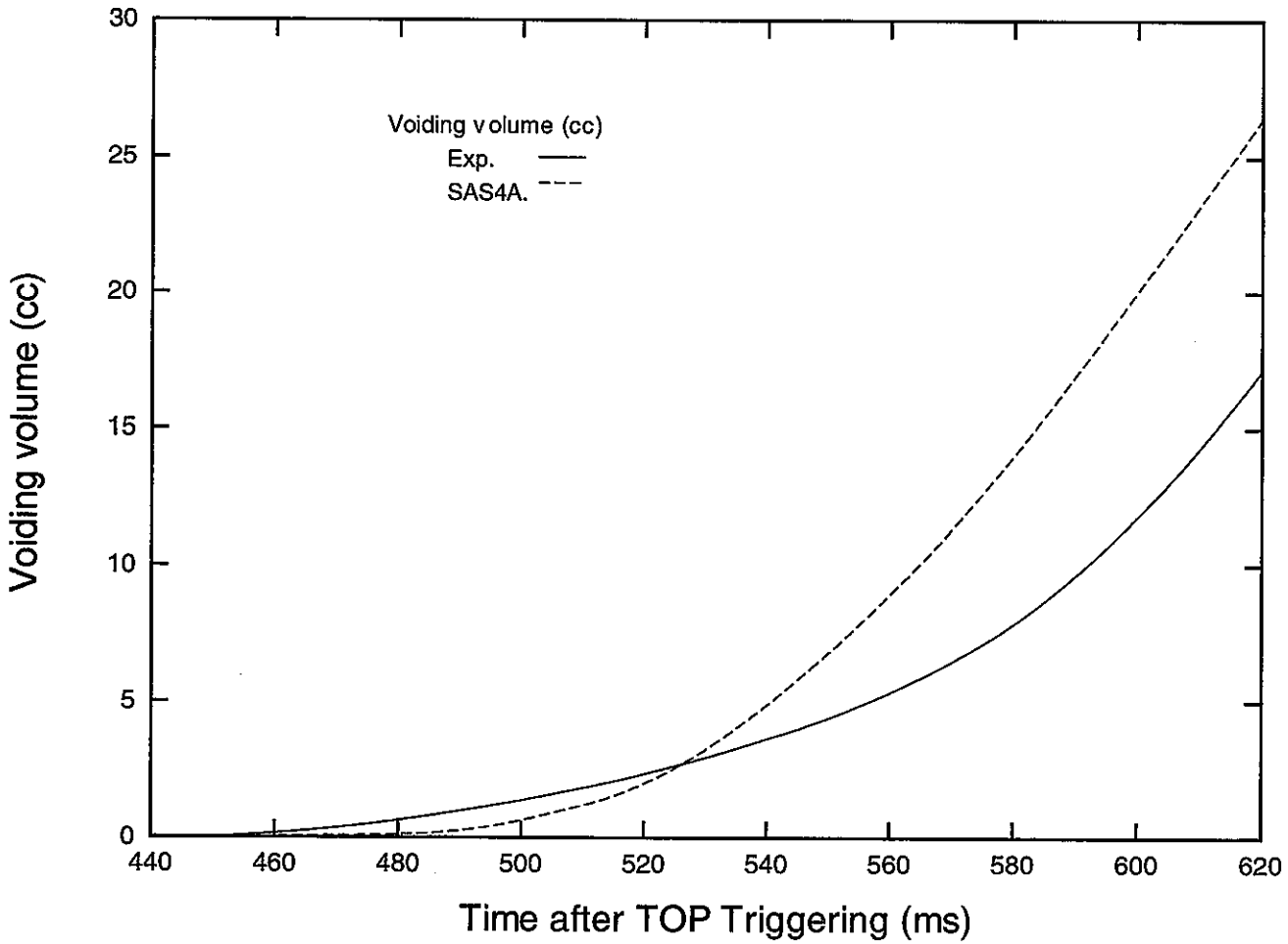

Fig.4-4 Voiding volume calculated from flow rate response

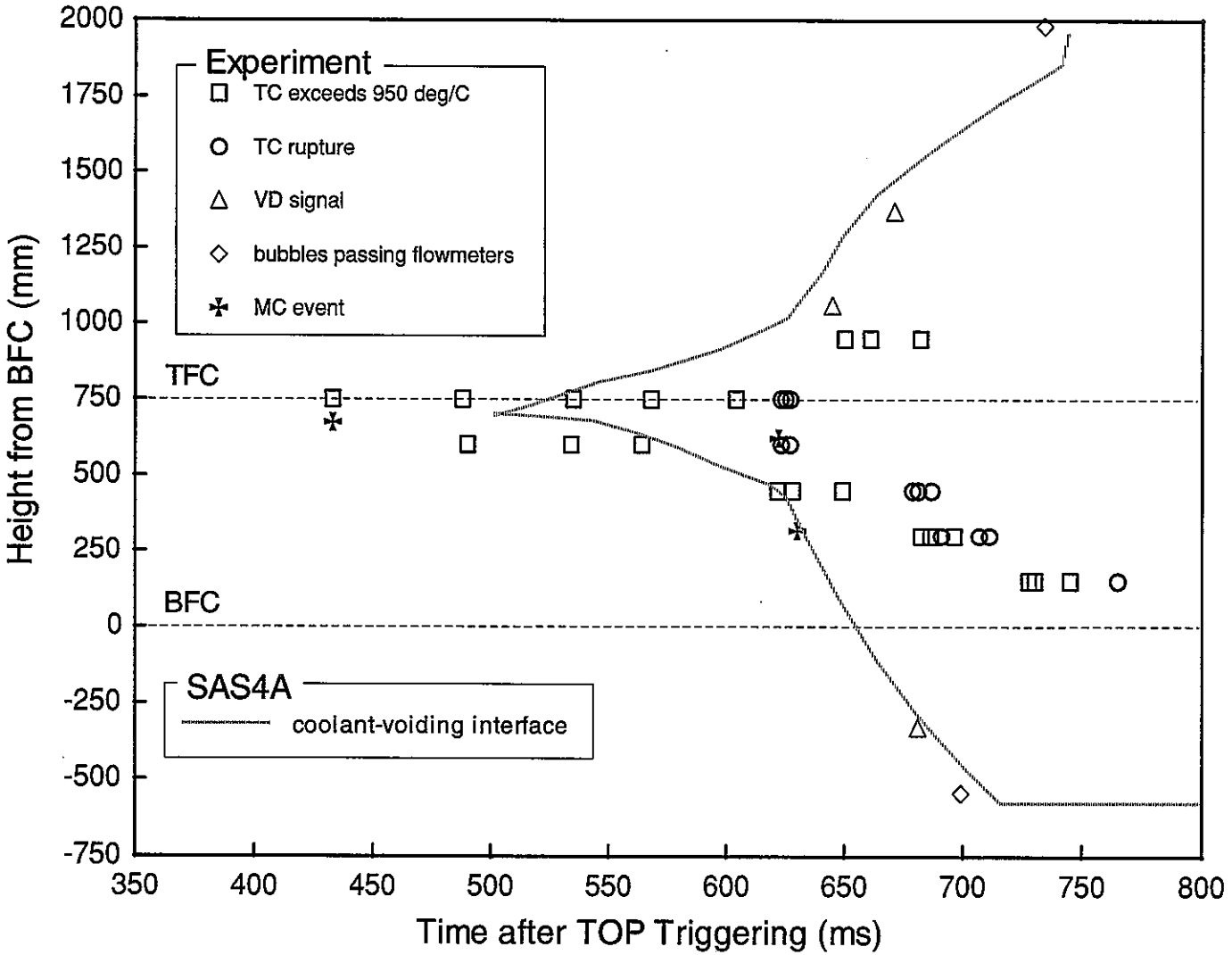

Fig.4-5 Development of coolant-voiding region

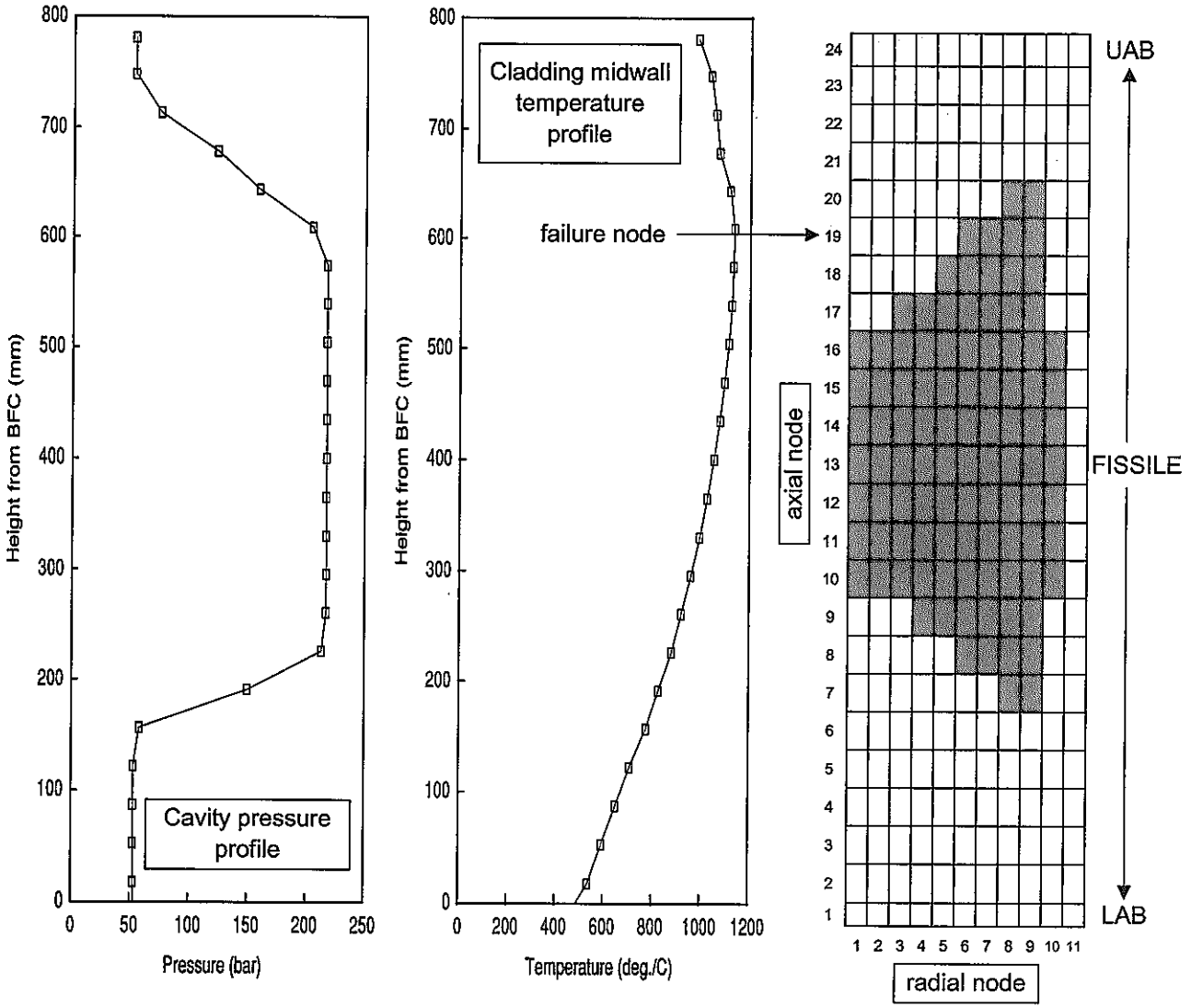

Fig.4-6 Calculated condition at observed failure
(cavity pressure, cladding temperature and fuel melting boundary)

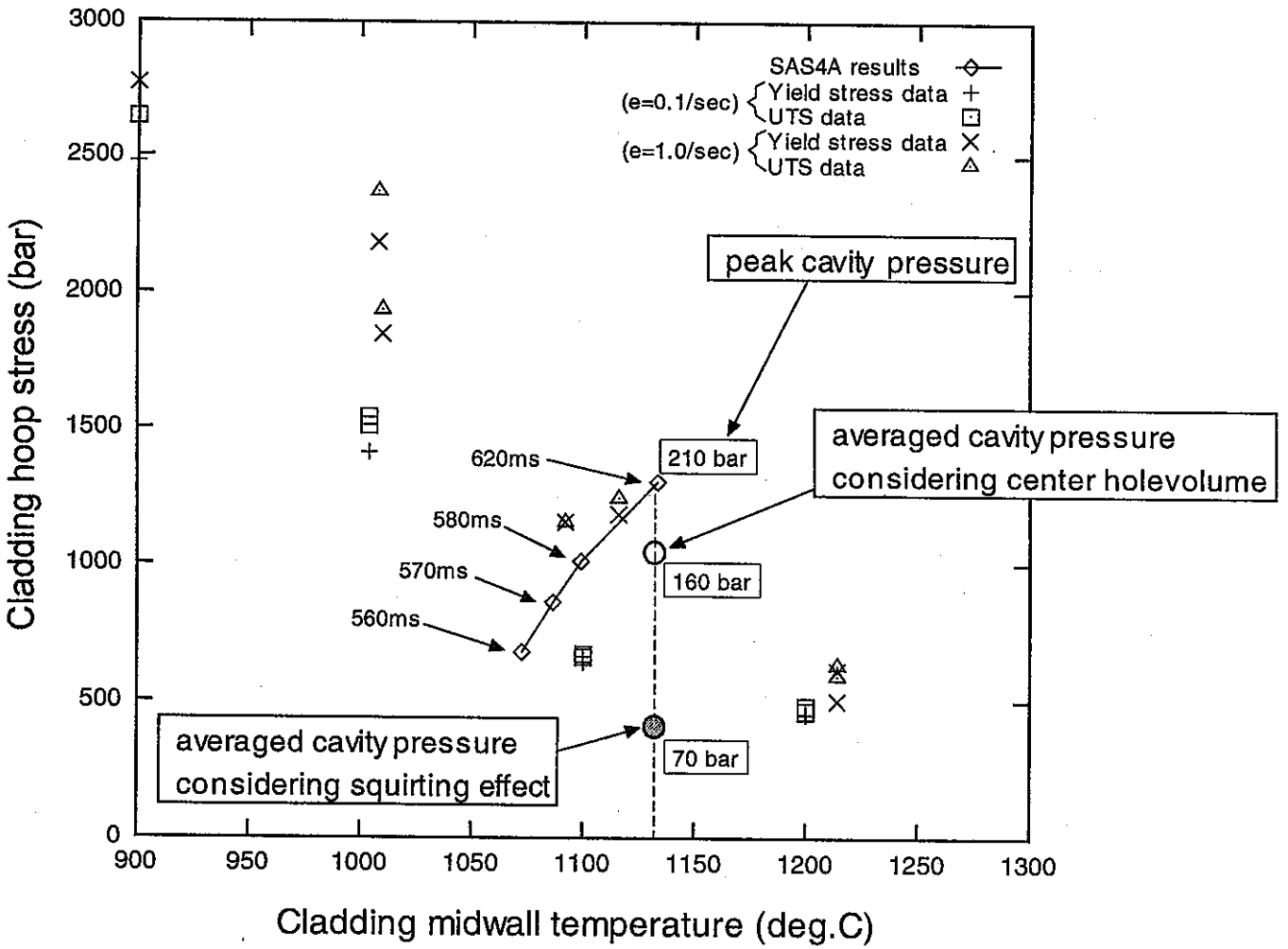

Fig.4-7 Cladding midwall temperature and hoop stress corresponding to cavity pressure at the observed failure location

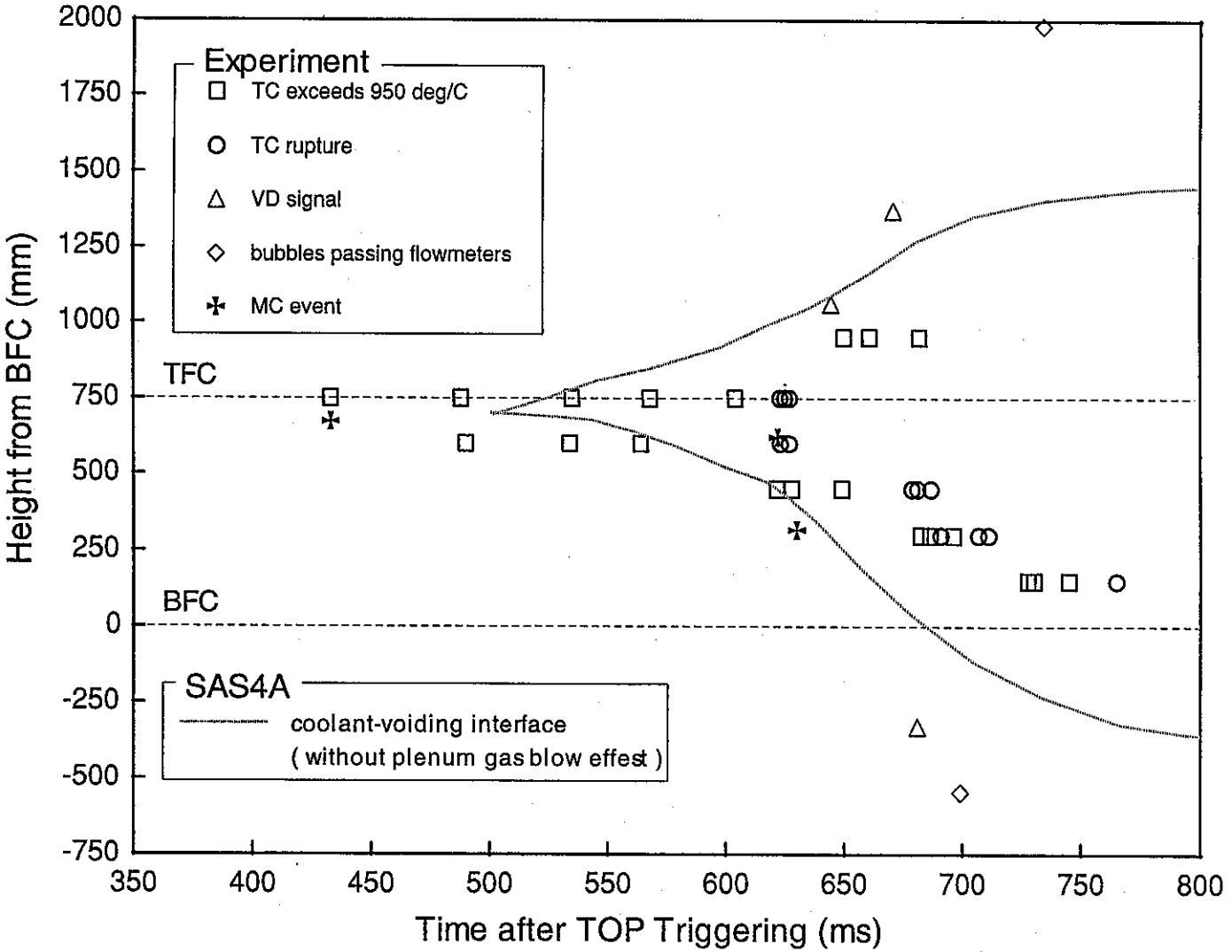

Fig.4-8 Development of coolant-voiding region

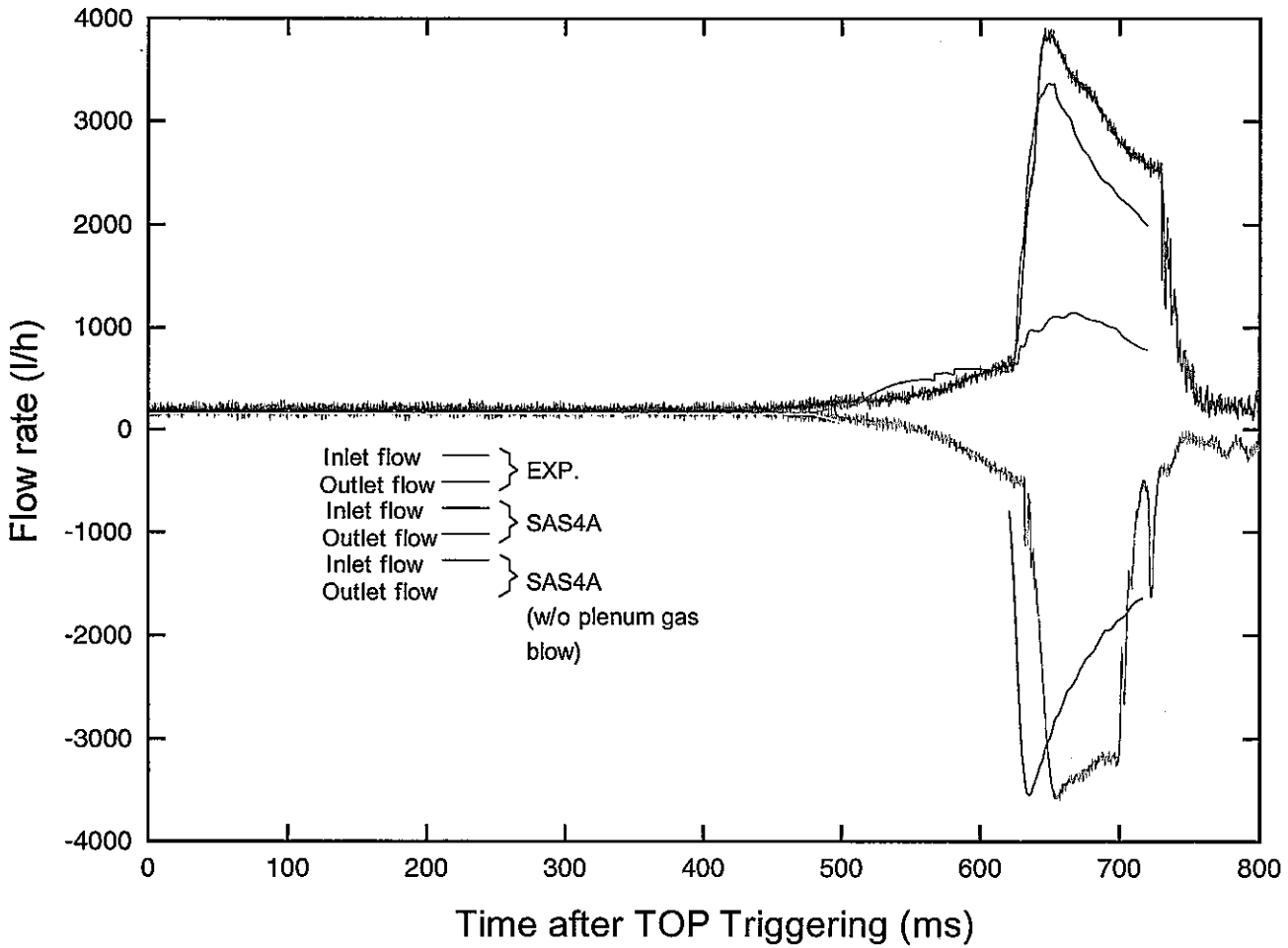

Fig.4-9 Comparison of coolant flow rate response during the TOP

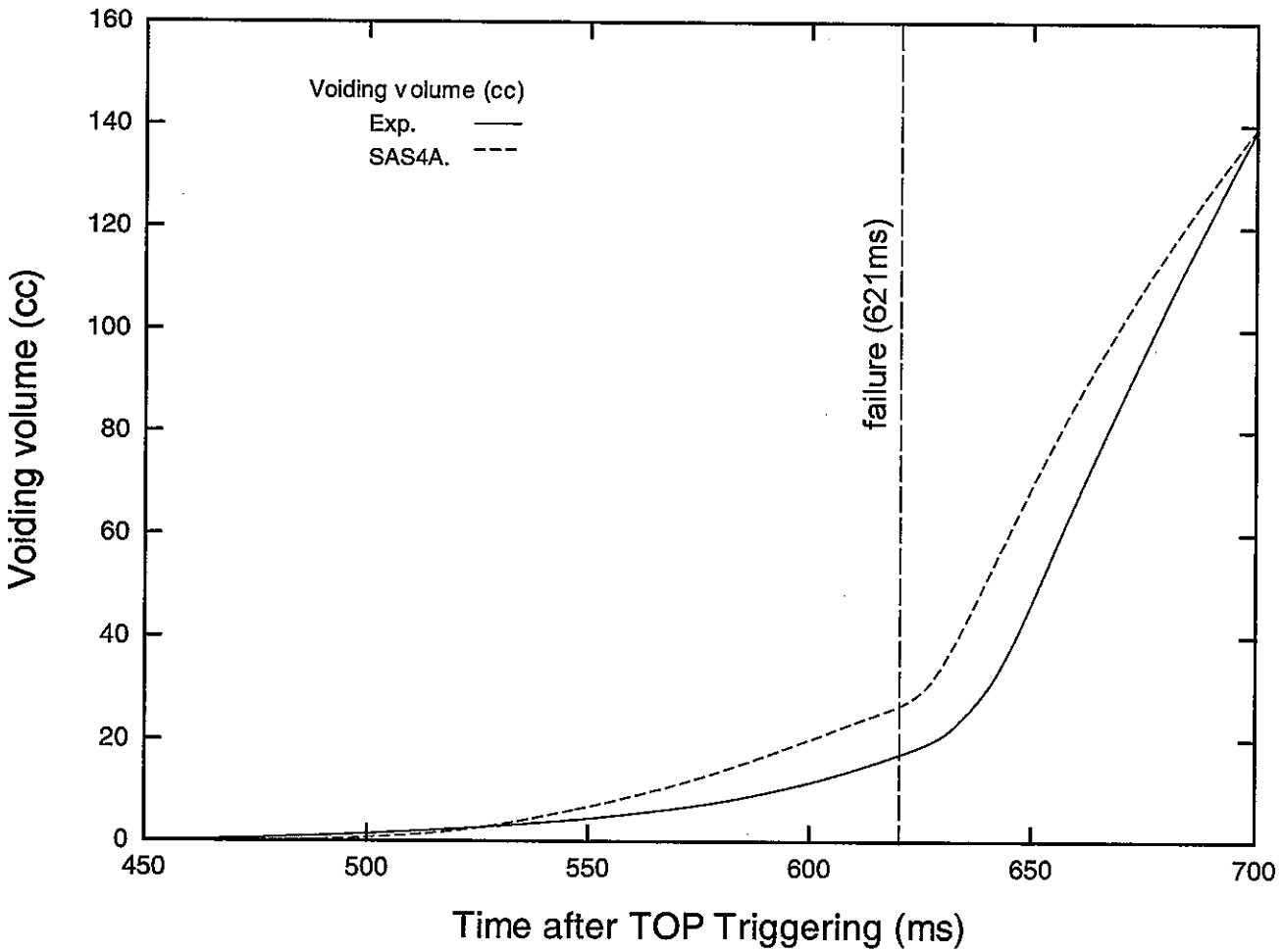

Fig.4-10 Voiding volume calculated from flow rate response

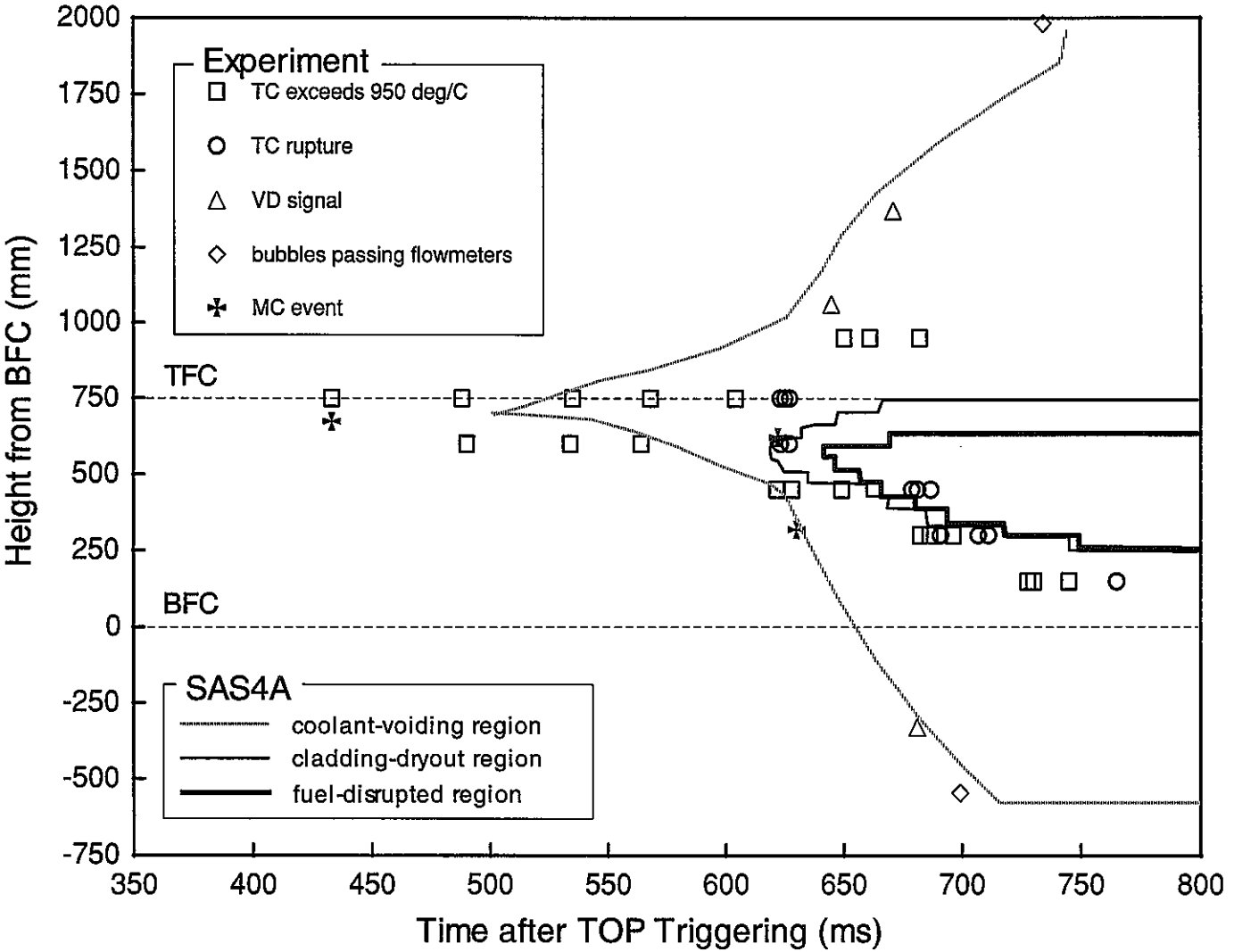

Fig.4-11 Development of coolant-voiding, cladding-dryout region and fuel disruption

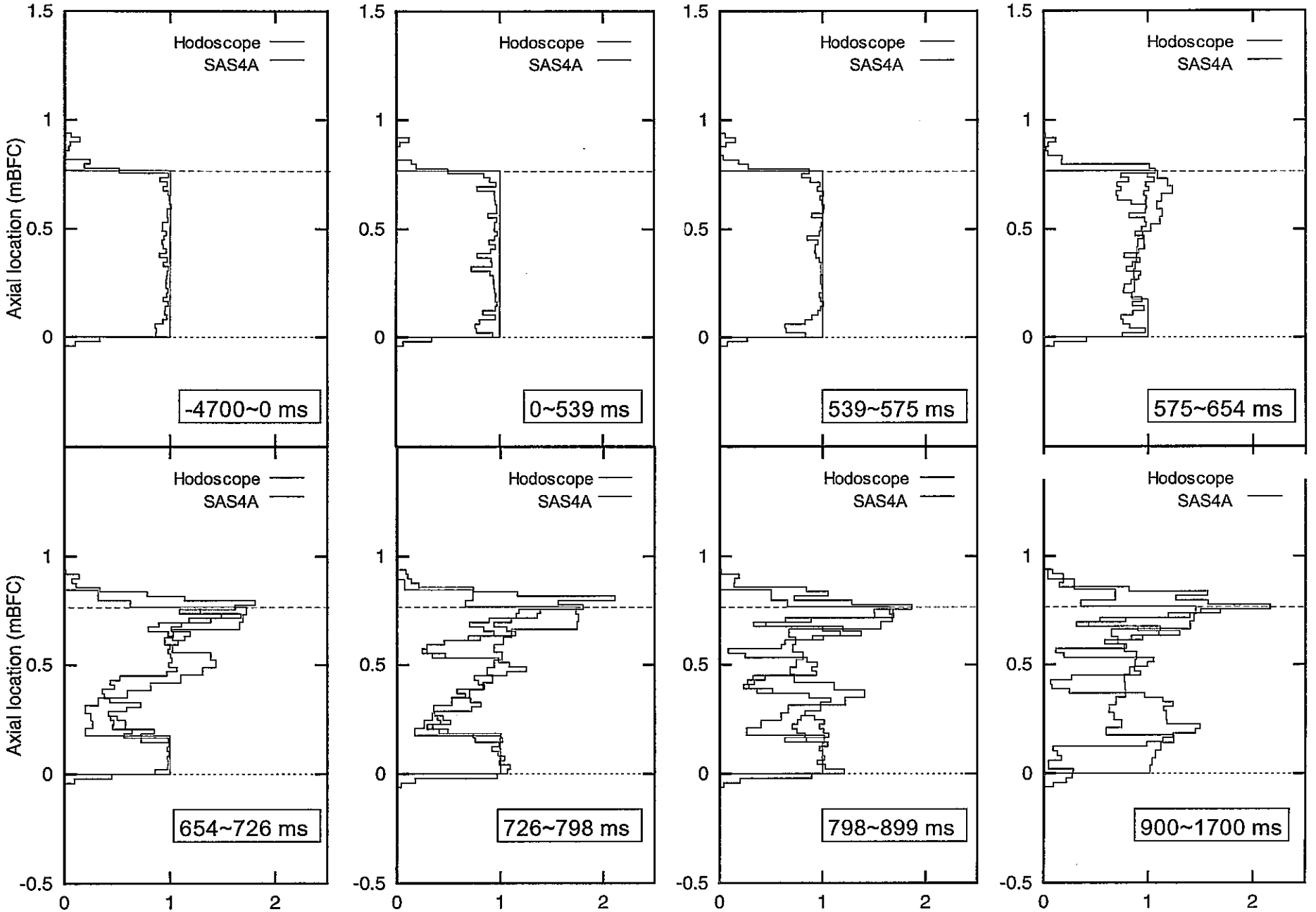

Fig.4-12 Normalized fuel mass distributions at different time intervals

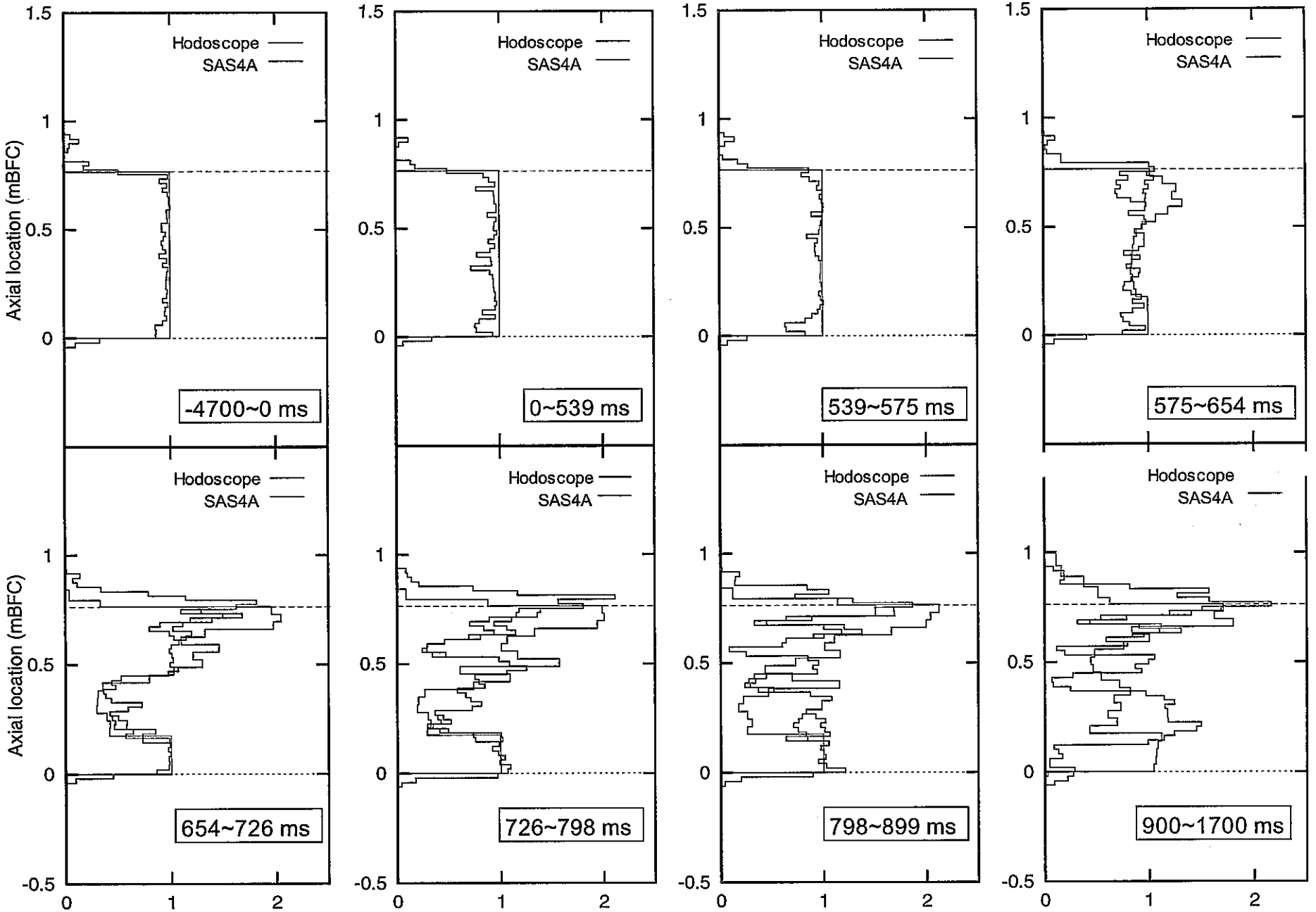

Fig.4-13 Normalized fuel mass distributions at different time intervals
(without plenum gas blowout effect)

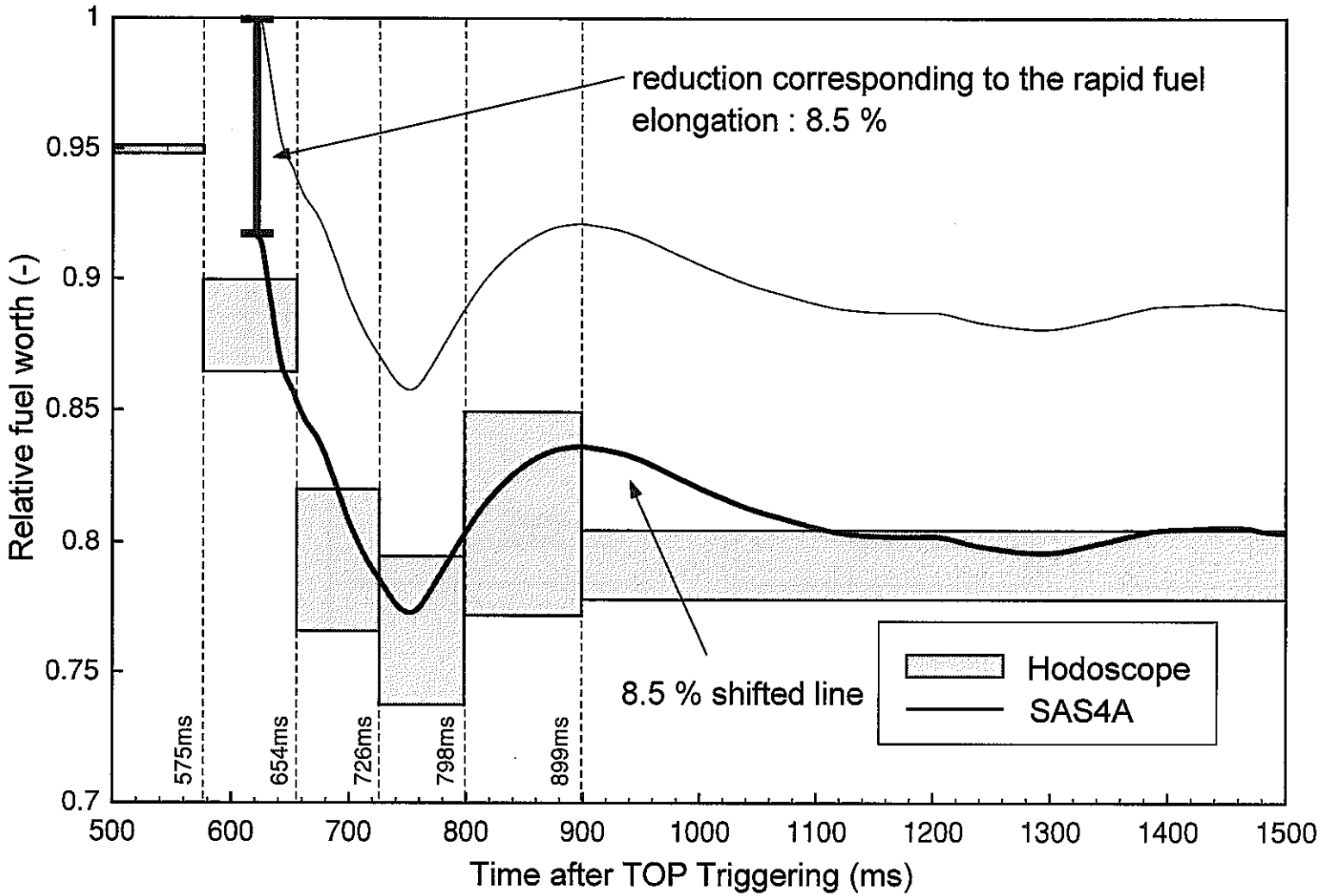

Fig.4-14 Histories of the relative fuel worth deduced from the hodoscope data and SAS4A result with correction for the rapid fissile elongation

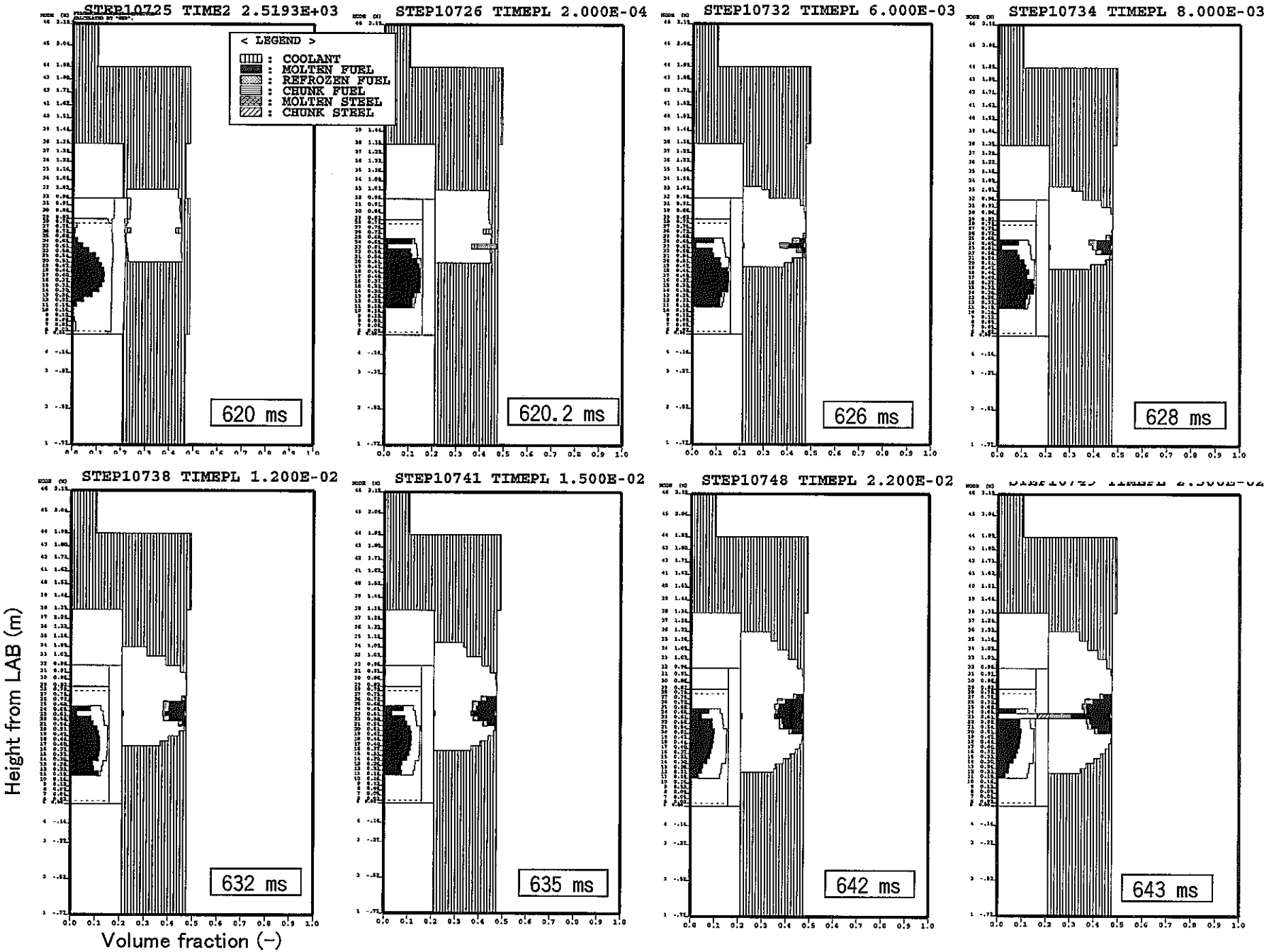

Fig.4-15 Volume fractions of the various components during the TOP

initial cavity pressure
: 210bar

initial cavity pressure
: 70bar

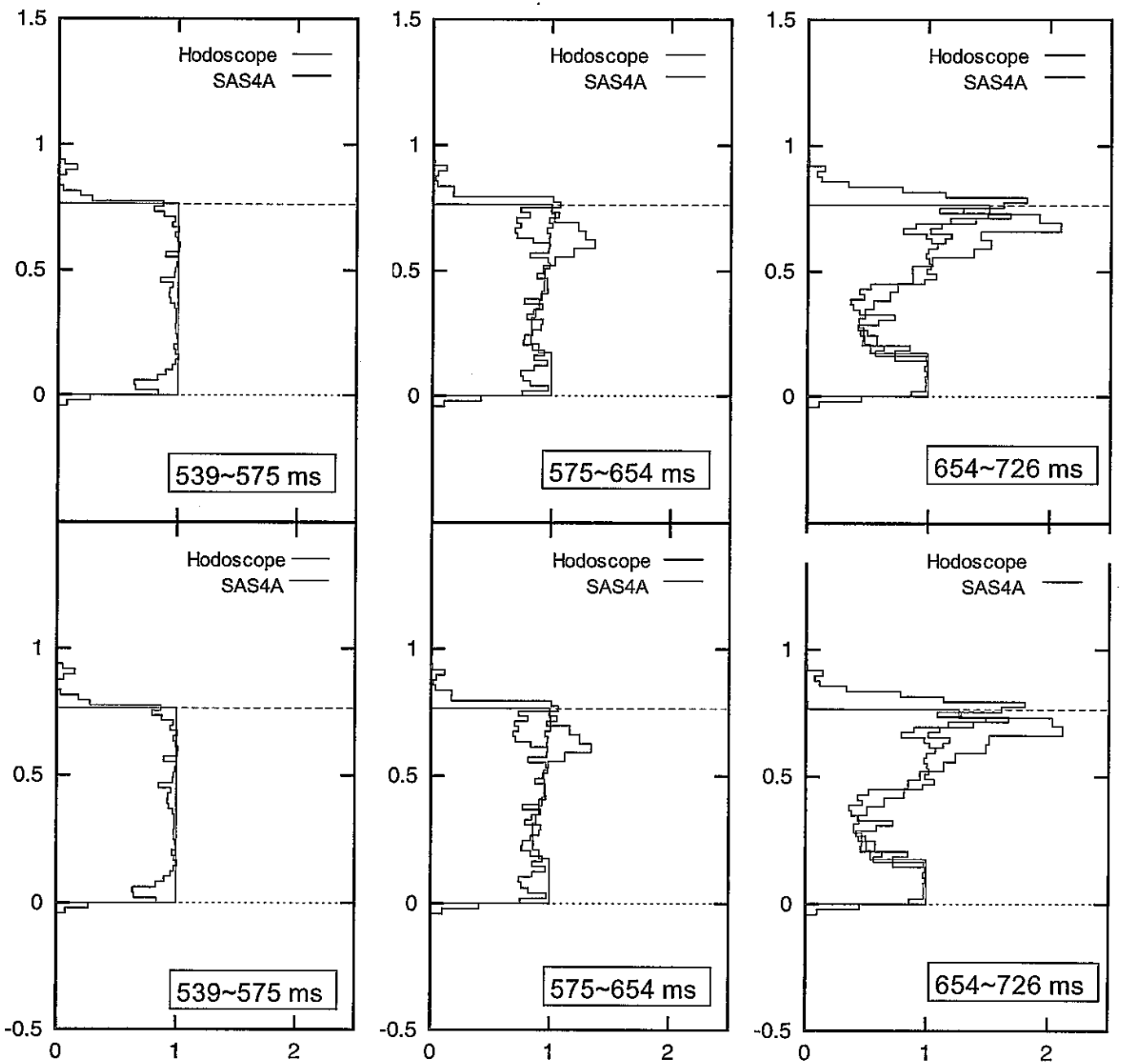

Fig.4-16 Comparison of fuel relocation behavior just after pin failure